AsPac J. Mol. Biol. Biotechnol. 2022
Vol. 30 (3) : 123-134

Development and characterisation of mouse monoclonal antibody against 'neonatal' Nav1.5

Nur Aishah Sharudin[a], Nur Amira Khairil Anwar[a], Muhamad Najmi Mohd Nazri[a], Ahmad Hafiz Murtadha[a], Fatin Hamimi Hamat@Mustafa[a], Maria Elena Sarmiento[b], Armando Acosta[b], Nik Soriani Yaacob[c], Noor Fatmawati Mokhtar[a*]

[a]*Institute for Research in Molecular Medicine (INFORMM), Universiti Sains Malaysia, Health Campus, 16150 Kubang Kerian, Kelantan, Malaysia*

[b]*School of Health Sciences, Universiti Sains Malaysia, Health Campus, 16150 Kubang Kerian, Kelantan, Malaysia*

[c]*Department of Chemical Pathology, School of Medical Sciences, Universiti Sains Malaysia, Health Campus, 16150 Kubang Kerian, Kelantan, Malaysia*

Received 24th March 2022 / Accepted 18th July 2022

Abstract. 'Neonatal' Nav1.5 (nNav1.5) is a potent tumour metastasis marker found especially in aggressive human breast cancer cells *in vitro*, in tumour tissues of *in vivo* metastatic animal models and in patients positive for lymph-node metastasis. Its expression has been recently described in human brain neuroblastoma and astrocytoma. However, a thorough understanding of nNav1.5's role in cancers has been limited by the lack of specific antibodies against it. Here, a mouse monoclonal antibody, 4H8 mAb-nNav1.5, was obtained and characterised concerning its efficacy in detecting nNav1.5 using indirect ELISA, surface plasmon resonance (SPR), Western blotting and immunofluorescence microscopy. 4H8 mAb-nNav1.5 was selected from a panel of hybridoma clones raised against nNav1.5 specific peptide (15 mers). The antibody exhibited linear association against nNav1.5 specific-linear peptide in indirect ELISA and was supported by SPR. The antibody also demonstrated strong immunoreactivity in immunofluorescence imaging of nNav1.5-abundant cells, human and mouse aggressive breast cancer cells, MDA-MB-231 and 4T1, respectively, which was not observed in nNav1.5-deficient cells, human less aggressive breast cancer cells, MCF-7 and non-cancerous breast epithelial cells, MCF-10A. This study demonstrates the initial description of 4H8 mAb-nNav1.5, which could serve as a beneficial tool to enhance future studies on nNav1.5 expression and function in cancers.

Keywords: nNav1.5, monoclonal antibody, breast cancer, ELISA, surface plasmon resonance, immunofluorescence microscopy

INTRODUCTION

Voltage-gated sodium channels (VGSC) mediate Na^+ ion influx and have a role in the initiation process of action potential in excitable cells such as neurons, myocytes, and cardiomyocytes (Hille, 2001; Terlau & Kirchhoff, 2006; Hucho, 2019). There are ten subtypes in the family of VGSC; Nav1.1 - Nav1.9 and Nax, and each could give rise to multiple variants due to either selective splicing of their mRNA or different modifications during the transcription process (Schroeter *et al.*, 2010). Nav1.1–1.3 and Nav1.6–1.9 support the electrical propagation in neurons, whereas Nav1.4 and Nav1.5 drive electrogenesis in skeletal muscle

*Author for correspondence: Noor Fatmawati Mokhtar, Institute for Research in Molecular Medicine (INFORMM), Universiti Sains Malaysia, Health Campus, 16150 Kubang Kerian, Kelantan, Malaysia. Email – fatmawati@usm.my

cells and cardiac myocytes (Black & Waxman, 2013).

Enhanced expression of VGSC has been detected in several types of human cancers, e.g., breast cancer, melanoma, prostate, lung, colon, ovarian, cervical, pancreatic, and gastric (Fraser *et al.*, 2005; Gazina *et al.*, 2010; Yang *et al.*, 2012; Xing *et al.*, 2014; Nelson *et al.*, 2015; Angus & Ruben, 2019; Guzel *et al.*, 2019; Mao *et al.*, 2019). Different carcinomas seem to express different subtypes of VGSC. However, two subtypes appear most common, Nav1.5 and Nav1.7 (Guzel *et al.*, 2019), where their canonical and non-canonical roles modulate the regulation of effector functions such as phagocytosis, motility, and other metastatic activities (Angus & Ruben, 2019; Guzel *et al.*, 2019; Mao *et al.*, 2019).

In aggressive breast cancer cell lines, such as MDA-MB-231, >80% of VGSC expression is contributed by Nav1.5, but subsequent sequence analysis revealed that the predominant variant is the 'neonatal' splice variant- nNav1.5 (Fraser *et al.*, 2005). Later, nNav1.5 expression was detected in tissues of metastatic animal models and breast tumour tissues positive for lymph node metastasis (Fraser *et al.*, 2005; Yang *et al.*, 2012; Nelson *et al.*, 2015). Interestingly, nNav1.5 has also been described in other cancer types such as human neuroblastoma and astrocytoma (Xing *et al.*, 2014).

nNav1.5 was identified as a D1:S3 5'-splice variant characterised by a highly conserved aspartate residue at the extracellular end of DI: S3, which was replaced by a positively charged lysine (Gazina *et al.*, 2010). The sequence of nNav1.5 differed from the adult at 31 of its 92 nucleotides, yielding 7 amino acid changes in the three species. The difference was considered a huge change compared to other α subunits of VGSC, which raised the possibility of generating an antibody specific to nNav1.5. For this reason, the first anti-peptide polyclonal antibody (pAb) against the region was raised in a rabbit, named NESOpAb, by a group of U.K. researchers (Chioni *et al.*, 2005). NESOpAb was immunoreactive against the neonate's heart and brain lysate but not the adult, as shown by Western blotting. Similarly, NESOpAb was immunoreactive against cell lines over-expressing nNav1.5, as shown by immunocytochemistry (Chioni *et al.*, 2005; Fraser *et al.*, 2005).

Later on, a monoclonal antibody (mAb) claimed to be anti-nNav1.5, catalogued as 4G8:1G7, was commercially made available by Abcam (U.K.) (Abcam, 2015). 4G8:1G7 was raised from a 14-amino acid immunogen which includes 6 amino acids specific for the neonatal variant. However, all the references claimed to have utilised 4G8:1G7 were used to detect Nav1.5 (and not nNav1.5) in cardiac cells (Guo *et al.*, 2011; Utrilla *et al.*, 2017; Vikram *et al.*, 2017). In another reference, rabbit pAb of anti-human Nav1.5 (Abcam, catalogue number was not mentioned) was utilised but claimed that nNav1.5 was detected in human astrocytoma (Xing *et al.*, 2014). All these confusing examples highlight the importance of nNav1.5 vs Nav1.5 and specific antibodies against nNav1.5 for research on the expression and role of nNav1.5 in disease pathology.

We recently obtained an anti-peptide mouse mAb-nNav1.5, 4H8, raised against a similar region as the rabbit polyclonal, NESOpAb. In this study, 4H8 mAb-nNav1.5 was characterised concerning its efficacy in indirect ELISA, surface plasmon resonance (SPR), Western blotting and immunofluorescence microscopy to demonstrate that 4H8 mAb-nNav1.5 could meet the requirements to study nNav1.5 expression in cells and tissue.

MATERIALS AND METHODS

Generation of mAb-nNav1.5

Conjugated peptide VSENIKLGNLSALRC with immunogenic carrier proteins, key-hole limpet hemocyanin (KLH) (Genscript, USA) (GenBank: CAC84535.1 - from biopsy sample of the breast cancer of *Homo sapiens*) was used as an immunogen. Five mice (two BALB/c, three C57BL/6) were immunised (four rounds) with nNav1.5 specific peptide (first round immunisation with KLH-conjugated peptide [50 μg] with Complete Freund's adjuvant (CFA), followed by booster injections on day 14, 28, and 50 with booster dosage of 25 μg formulated with Incomplete Freund's adjuvant (IFA) each time). The animals were bled and sacrificed on day 57. The animal sera were collected and subjected to selection for antibody response using indirect

ELISA. Spleen cells from the mice with the highest absorbance for serum antibody response (indirect ELISA) were fused with myeloma cells to produce hybridomas. Hybridomas were cultured and sub-cloned by limiting dilution. Supernatants were assayed after cell fusion, and wells with confluent hybridomas were initially screened by ELISA (Genscript, USA). Finally, 20 hybridoma clones were obtained, and their supernatants were collected and further selected by ELISA and Western blotting. The selected clone was purified using one-step purification Protein-A resin (recombinant protein A coupled to 4% agarose) (Genscript, USA).

Cell culture

Human breast cancer cell lines, MDA-MB-231 and MCF-7, non-cancerous human breast epithelial cell line, MCF-10A and mouse mammary cancer cell line, 4T1 cells were obtained from the American Type Culture Collection (ATCC, USA). The MDA-MB-231, MCF-7 and 4T1 were cultured in Dulbecco's Modified Eagle's Medium (DMEM) (Nacalai Tesque, Japan) supplemented with fetal bovine serum (5%) and L-glutamine (4 mM), whilst MCF-10A cells were cultured in DMEM/F12 (Nacalai Tesque, Japan) supplemented with 5% horse serum, epidermal growth factor (100mg/ml), hydrocortisone (100 mg/ml), cholera toxin (1 mg/ml) and insulin (10mg/ml). All cells were maintained at a constant temperature of 37°C in a 5% CO_2 and relative humidified atmosphere. Cells were passaged when the confluency reached 80%.

Orthotopic syngeneic tumor model

Animal experiments were approved by the Animal Ethics Committee of Universiti Sains Malaysia (USM) following their relevant regulatory standards (USM/IACUC/2018/ (113) (934)). Under light anaesthesia, the fur of the mice was shaved over the lateral thorax. The 4T1 cells of volume 0.1 ml (5 x 10^5 cells) were subcutaneously injected into the mammary fat pads by gently penetrating the skin of the mice. The onset of the primary mammary tumour was monitored daily by palpating the injection area with the index finger and thumb for its presence, which usually develops within one week. Their tumour volume was measured twice a week using a Vernier calliper and calculated using the following formula $ab^2/2$, (a = length of tumour, b = width of tumour). The mouse was sacrificed when the tumour reached 14 to 16 mm (approximately four weeks post-injection) or when the mice became moribund. Animals were anaesthetised with sodium pentobarbital (200 mg/kg) (Vetoquinol, UK), and the mammary tumours were collected and subjected to protein extraction.

Western blotting

Protein was extracted from tumour tissues of an orthotopic animal mouse model and cell lysates of 4T1 and MDA-MB-231 (~80% confluency) using RIPA buffer (Thermo-Fisher Scientific, USA). Protein extracts were separated by 7.5% comparative SDS-PAGE at 90V for 90 minutes and electro-blotted onto the nitrocellulose membrane at 15V for 105 minutes. After transfer, blots were blocked at room temperature (20 - 22°C) for one hour with gentle agitation in a 1% (w/v) solution of non-fat dried milk in distilled water and Tween-20. Blots were then probed with primary antibodies; hybridoma cell supernatants (undiluted), #7435 immunised serum (1:300), mAb-nNav1.5 (1:10) and commercialised Nav1.5 polyclonal antibody (Santa Cruz Biotech, USA), diluted in 1% blocking solution at 4°C overnight. Internal 'loading' control was β-Actin (1:500) (Santa Cruz Biotech, USA). The blots were washed with Tris-buffered saline (four times), followed by a one-hour incubation with secondary antibody (horseradish peroxidase-conjugated) (Santa Cruz Biotech, USA) at room temperature (20 – 22°C). Blots were washed for 3 x 10 minutes, and bands were visualised using a Chemi-Lumi One kit (Nacalai Tesque, Japan).

Indirect ELISA

ELISA plates (Microloan 600, high binding F-bottom) were coated with 100 µL/well of 4 µg/mL nNav1.5 short-linear peptide overnight at 4°C in coating buffer (phosphate-buffered saline [PBS], pH 7.4). The unbound antigens were discarded by washing four times with 1X PBS, 0.2% Tween-20, pH 7.5. The plates were incubated at 37°C for one hour with a blocking buffer (5% skimmed milk, 1X PBS, 0.2% Tween-20). 4H8 mAb-nNav1.5 was diluted in series of concentration; 1000, 500, 250, 125, 62.50, 31.25, 15.62, 7.81, 3.90 and 1.95 ng/ml in 1X PBS (1:2),

incubated at 37°C for one hour, followed by incubation with secondary, goat anti-mouse IgG (1:10,000) (Origene, USA) at 37°C for one hour. After the solution was removed, each well was washed four times with the washing solution, and 100 µL of 3,3',5,5'-Tetramethylbenzidine (TMB) was then added to the wells. The enzymatic reaction was stopped by adding 100 µL of 2 M H_2SO_4 (Merck, Germany). The intensity of the resulting yellow colour was measured spectrophotometrically at 450 nm. 'Adult' Nav1.5 free-peptide AYTTEFVDLGNVSALR (Bio Basic, Singapore) in a 1 µg/mL concentration was used as a negative control.

Surface plasmon resonance (SPR)

Binding kinetics and binding affinity between 4H8 mAb-nNav1.5 and nNav1.5 specific-linear peptides were performed using SPR (Biacore X100-Plus, GE Healthcare, Sweden). A sensor chip CM5 (G.E. Healthcare, Sweden) carrying a carboxymethylated dextran matrix was activated using amine coupling (ECD/NHS ratio 1:1). Then, the activated sensor chip immobilised 30 µg/mL of 4H8 mAb-nNav1.5 in sodium acetate solution (10 mM, pH 5.0). This was followed by an injection of 10 mM ethanolamine to block unused carboxylic terminals. Kinetic and affinity analyses were performed by flowing nNav1.5 specific peptide at the rate of 30 µL/min along with the flow cell in five serial dilutions of 10, 5, 2.5, 1.25, and 0.625 µg/mL dissolved in 1X PBS, pH 7.4. The contact time, 120 and 600 seconds, was allocated for dissociation time by multi-cycle kinetic setting. The sensor chip was then regenerated using ten mM Glycine-HCI, pH 2.5 after each dissociation phase of the respective concentration for 30 seconds. 'Adult' Nav1.5 short-linear peptide AYTTEFVDLGNVSALR (Bio Basic, Singapore) in a 1 µg/mL concentration was used as the negative control.

Immunofluorescence microscopy

Cells with a seeding density of 3 X 10^4 were grown on the plastic coverslip (Thermo Fisher Scientific, USA) and then fixed with cold acetone. Concanavalin A solution (ConA) (Sigma-Aldrich, USA) (1:10 dilution in 1 X PBS) was put on top of coverslips in an incubation chamber and left on a rocker platform for 45 minutes in the dark. Permeabilization buffer (0.2% Triton-X100, 2% BSA) was added to each sample prior to primary antibody incubation (1 hour) with 4H8 mAb (1:100) or commercialized anti-Nav1.5 mAb (Santa Cruz Biotech, USA) (1:50) that was diluted in antibody signal enhancer (10 mM glycine, 0.05% Tween-20, 0.1% Triton X-100, 0.1% hydrogen peroxide in PBS) (Rosas-Arellano *et al.*, 2016). The secondary antibody used was Cruz Fluor (SC-516177) conjugated monoclonal anti-mouse IgG (Santa Cruz Biotech, USA). Coverslips were mounted on Fluoro-Keeper anti-fade reagent with DAPI (Nacalai Tesque, Japan). Imaging was done using Leica Inverted DMi8 Fluorescence and captured using DFC 365 FX Camera (Leica Microsystems, Germany).

Quantitative real-time reverse transcription-polymerase chain reaction (qRT-PCR) analysis

In this study, human and mouse (cells and tissues) were used as samples. In order to confirm the presence of nNav1.5 in these two species, qRT-PCR was conducted. Briefly, total RNA was extracted using the Sepasol method according to the protocol provided by the manufacturer (Nacalai Tesque, Japan). According to the manufacturer's protocol, 1 µg of total RNA was converted to cDNA using ReverTra Ace® qPCR RT Master Mix with gDNA Remover (Toyobo, Japan). According to the manufacturer's protocol, real-time PCR was performed using triplicates using the SensiFAST SYBR Hi-ROX kit (Bioline, UK). Sequence primers used were as follows:

Table 1. Primers used in this study.

Primer	Sequence	Source
B-actin forward	5'-ATTGCCGACAGGATGCAGAAG-3'	(Kamarulzaman *et al.*, 2017)
B-actin reverse	5'-TAGAAGCATTTGCGGTGGACG-3'	
nNav1.5 mouse forward	5'-TGGCGTATGTATCAGAGAATATAAAGC-3'	(Accession number NM_021544.4)
nNav1.5 mouse reverse	5'-CTGGAATAACTGAAATCGTTTTCAGAGC-3'	
nNav1.5 human forward	5'-CTGCACGCGTTCACTTTCCT-3'	(Accession number NM_001354701.1)
nNav1.5 human reverse	5'-GACAAATTGCCTAGTTTTATATTT-3'	

Quantitative real-time was performed in an ABI Prism 7000 Sequence Detection System (Life Technologies, USA). The amplification condition was set as follows: initial activation for 5 min at 95°C for one cycle, 10 s at 95°C, and 30 s at 60°C for 35 cycles. Ct values of target genes were normalised to β-actin, and the relative mRNA expression of target genes was calculated by the $2^{-\Delta Ct}$ method.

Data analysis

All quantitative data were analysed using GraphPad Prism statistical software version 7.0. Linear regression with a 95% confidence interval described the linear relationship between variables interpreted with the R-squared value. Tukey's Multiple Comparison Test compared nNav1.5 protein expression between cell lines. Meanwhile, Leica Application Software X (LAS X) was used to analyse imaging studies.

RESULTS

Selection of animal and hybridoma positive for anti-nNav1.5

Five mice (two BALB/c; #7431, #7432, three C57BL/6; #7433, #7434 and #7435) were immunised (four rounds) with nNav1.5 specific peptide (Figure 1A). Animal sera were collected, and indirect ELISA was conducted to assess serum antibody response on an ELISA plate coated with nNav1.5 peptide (4 µg/ml, 100 µl/well). Serum from animal C57BL/6; #7435 reacted strongly with the highest absorbance reading at 1.367 (Figure 1B). Serum antibody response for the immunised #7435 was compared to its pre-immune serum (Figure 1C) and proceeded with spleen extraction and monoclonal antibody production. The splenocytes were fused to 20 hybridoma cell lines, and supernatants from each cell/clone were collected.

Indirect ELISA was conducted in the primary screening of the 20 hybridoma clones on an ELISA plate coated with nNav1.5 peptide (4 µg/ml, 100 µl/well). All supernatants reacted strongly with an absorbance value read at 450 nm O.D. >1.5 (Figure 1D).

Supernatants were examined for their immunoreactivity in tumour tissue lysates and 4T1 and MDA-MB-231 cell lysates using Western blotting. Five supernatants (3H9, 4H8, 6H9, 11H8, and 13C6) immunoreacted (but not specifically produce the expected protein band) by producing protein bands (result not shown). In the second round of Western blotting with the five supernatants, only 4H8 reacted (again not specifically producing the expected protein band) (Figure 1E), hence proceeded to antibody purification, and the purified 4H8 was selected as mAb-nNav1.5.

Immunoreactivity of 4H8 mAb-nNav1.5 against nNav1.5 specific-linear peptide

Indirect ELISA was used to assess 4H8 mAb-nNav1.5 immunoreactivity against nNav1.5 specific-linear peptides. Results indicated that 4H8 mAb-nNav1.5 produced higher absorbance than the control blank and a linear regression line with $R^2 = 0.9707$ (Figure 2A and 2B), whilst titration of 4H8 mAb-nNav1.5 with the negative control, 'adult' Nav1.5 resulted in no signal detection (Figure 2C).

Molecular interaction analysis using SPR showed a value of disassociation rate, K_{off} was lower than that of the association rate, K_{on} with 0.004095 compared to 527.6, showing the longer time taken to unbind the antibody from the nNav1.5 peptide after binding (association) (Figure 3A). The result further showed a linear relationship between the response unit (R.U.) of 4H8 mAb-nNav1.5 against the concentration of nNav1.5 specific-linear peptide (in log 10) with high linearity correlation at $R^2 = 0.9887$ (Figure 3B). For kinetic analysis, nNav1.5 specific-linear peptide rapidly associated and dissociated to 4H8 mAb-nNav1.5 on the sensor chip. The R.U. yielded a dissociation constant (K.D.) of <40 pM. Injection of increasing concentrations of nNav1.5 specific-linear peptide resulted in an additional increase in R.U., with rapid dissociation during the experiment (Figure 3C). This observation indicated that the binding sites of 4H8 on nNav1.5 were direct and without any significant overlapping sites. Negative control of 'adult' Nav1.5 specific-linear peptide yielded below zero response unit (Figure 3D) with kinetic parameters indicating no binding with the 4H8 mAb-nNav1.5 on the sensor chip (Figure 3E).

Adult Nav1.5	Y T T E F V D L G N V S A L R T F R V L R A L K T I S V I S
Neonatal Nav1.5	Y V S E N I K L G N L S A L R T F R V L R A L K T I S V I P **C**

(A)

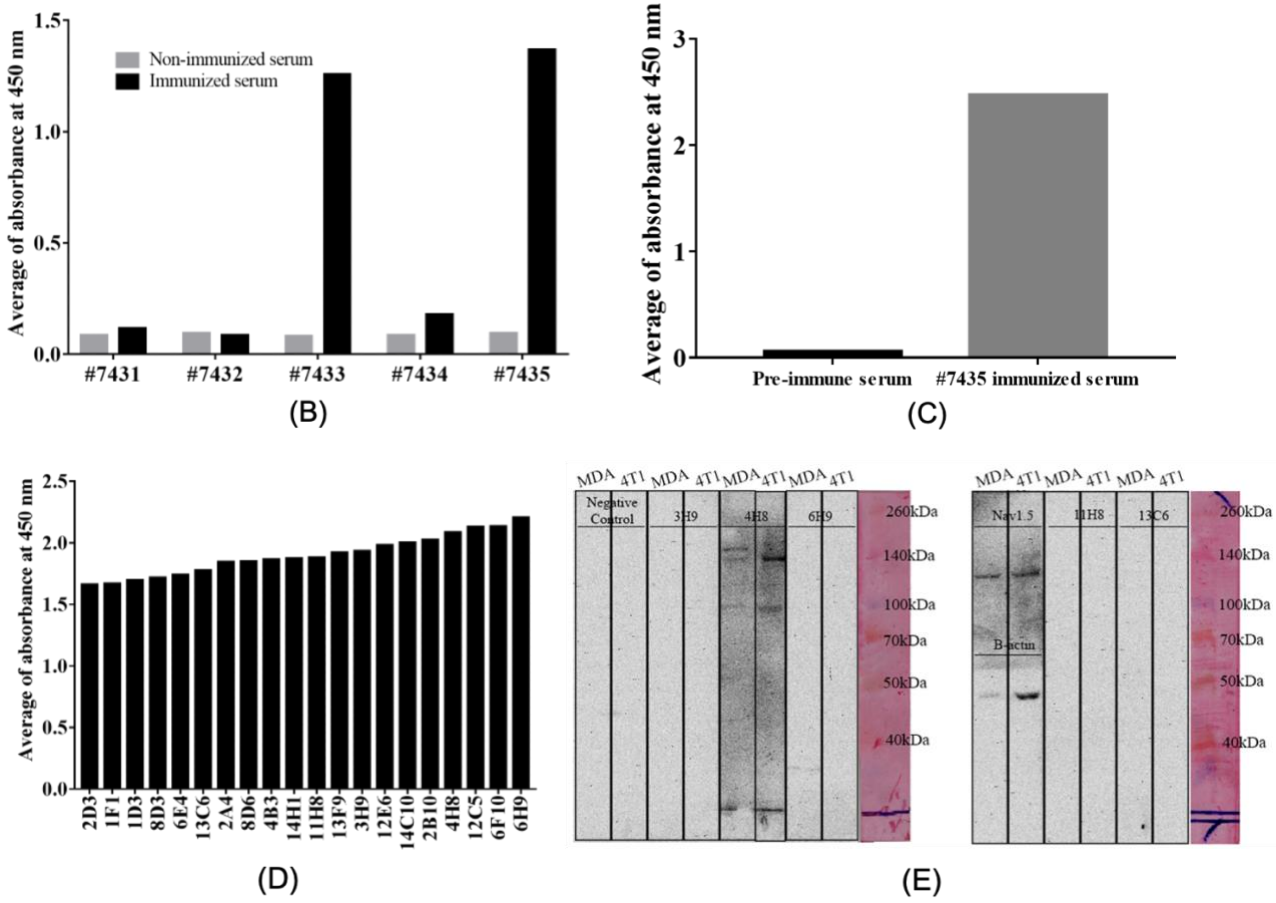

Figure 1. Selection of positive hybridoma for anti-nNav1.5. (A) The amino acid sequence difference between adult and neonatal Nav1.5 (underlined). The bold letter represents the added Cysteine, '**C'** amino acid to facilitate conjugation. (B) Animal serum antibody response after immunisation was measured with ELISA. (C) Serum antibody response of pre-immune vs #7435 immunised-serum measured with ELISA. (D) Antibody titer of 20 supernatants of the parental hybridoma was measured with ELISA. The plate was coated with nNav1.5 specific peptide (4 μg/mL, 100 μL/well) and 1 μg/ml negative control, incubated with supernatants and developed with TMB. The absorbance reading is the average of two technical replicates, read at OD 450nm. All values are expressed as the mean ± SEM for two independent experiments. (E) The 4H8 mAb-nNav1.5 failed to produce a specific protein band with approximate size for nNav1.5 (>220 kDa).

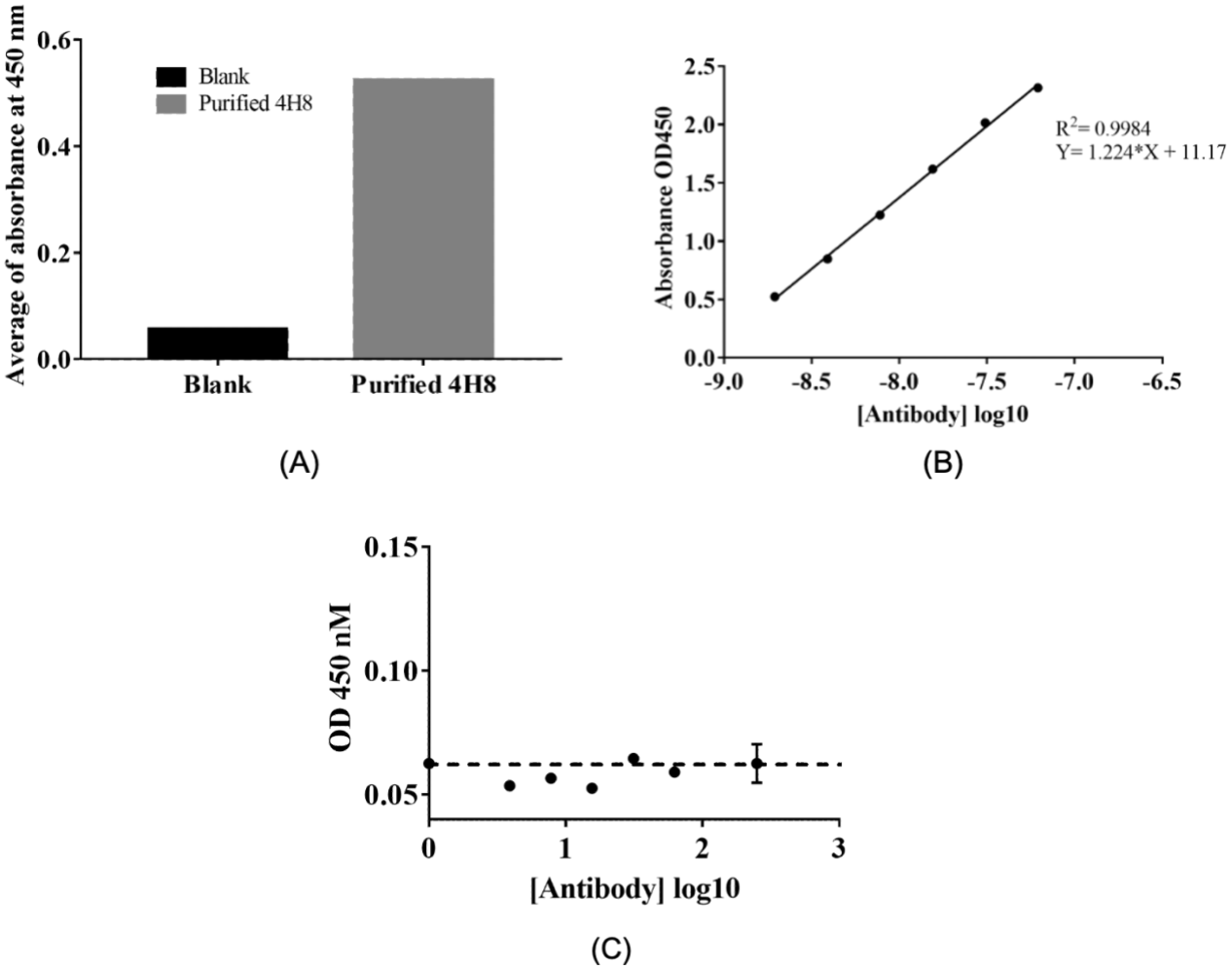

Figure 2. Characterisation of the purified 4H8 mAb-nNav1.5 by ELISA. (A) Antibody titer of purified 4H8 mAb-nNav1.5. (B) Linear regression analysis of purified 4H8 mAb-nNav1.5 measured using indirect ELISA. (C) Purified 4H8 mAb-nNav1.5 against negative control (adult Nav1.5 peptide) measured using indirect ELISA. The plate was coated with nNav1.5 specific peptide (4 µg/mL, 100 µL/well) and one µg/ml negative control (adult Nav1.5), incubated with 4H8 mAb-nNav1.5 and developed with TMB. The absorbance reading is the average of two technical replicates, read at OD 450nm.

K_{on}	527.6
K_{off}	0.004095

(A)

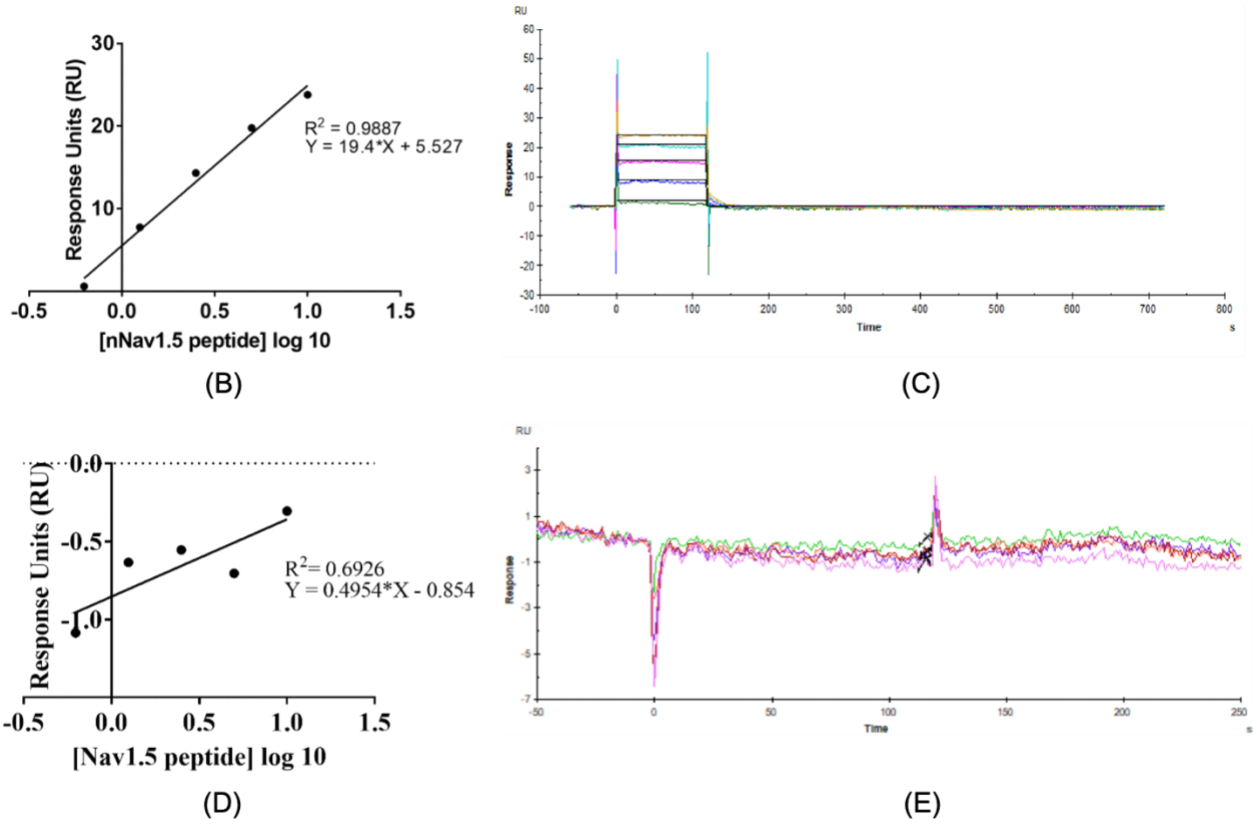

Figure 3. Binding affinity and kinetic parameter of the 4H8 mAb-nNav1.5 assessed via SPR sensor response. (A) Value of specific binding (K_{on} and K_{off}). Linear regression analysis (B) and dissociation curve (C) of nNav1.5 specific-linear peptide. Linear regression analysis (D) and dissociation curve of Nav1.5 specific-linear peptide - negative control (E). The R.U. falls below zero with no linear correlation indicating no binding between 4H8 mAb-nNav1.5 and the negative control of Nav1.5 specific-linear peptide.

mRNA expression of nNav1.5 in human breast cancer cells and mouse mammary tumour

In order to confirm the presence of nNav1.5 in human and mouse, qRT-PCR was conducted. Results revealed that both MDA-MB-231 and 4T1 expressed significantly higher expression of nNav1.5 than MCF-7 (Figure 4A).

Immunoreactivity of 4H8 mAb-nNav1.5 against nNav1.5 in cell and tissue lysates

Western blotting was conducted to assess 4H8 mAb-nNav1.5 immunoreactivity against lysates of cells/tissue; 4T1, MDA-MB-231, and mammary tumour tissue. However, results indicated the mAb-nNav1.5 unable to produce bands at approximate molecular mass for nNav1.5 of more than 220 kD (Figure 4B).

Immunoreactivity of 4H8 mAb-nNav1.5 in fixed cells

4H8 mAb-nNav1.5 produced a markedly different fluorescence intensity in different cell types. Strong intensity of red fluorescence was observed in nNav1.5-abundant cells, aggressive human breast cancer MDA-MB-231 and mouse mammary carcinoma, 4T1 cells (Figure 5A). On the other hand, fluorescence staining in nNav1.5-

deficient cell lines, the less aggressive human breast cancer cell lines, MCF-7 and non-cancerous human breast epithelial cells, MCF-10A, was not visible (Figure 5A). Imaging analysis revealed that the red fluorescence intensity was significantly higher in nNav1.5-abundant cell lines than in nNav1.5-deficient cell lines (Figure 5B). A similar red fluorescence signal was observed with the commercial anti-Nav1.5 mAb (Santa Cruz Biotech, USA) (Figure 5B), with a statistical difference observed between the expression of nNav1.5 & Nav1.5-abundant cell lines with nNav1.5 and Nav1.5-deficient cell lines in both 4H8 mAb-nNav1.5 and the commercial anti-Nav1.5 mAb.

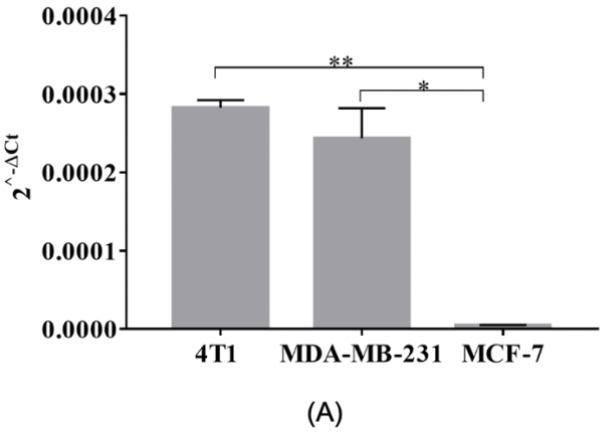

(A)

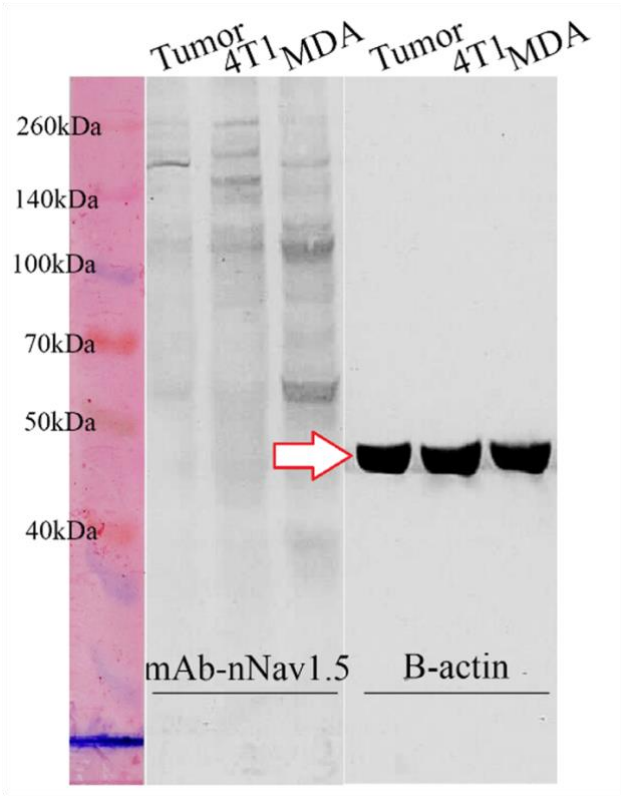

(B)

Figure 4. (A) MDA-MB-231 and 4T1 expressed significantly higher expression of nNav1.5 compared to MCF-7. The relative mRNA expression was measured using qRT-PCR, where β-actin was used as a housekeeping gene, and data were collected from n=3 independent experiments, presented as mean ± SEM. Tukey's Multiple Comparison Test was used, $p<0.01$, ** was considered statistically significant. (B) Western blot of tumour and cell lysates of 4T1 and MDA-MB-231 immuno-stained with 4H8 mAb-

nNav1.5 unable to produce bands at approximate 220kDa normalised with ß-actin (42 kDa) (marked with arrow).

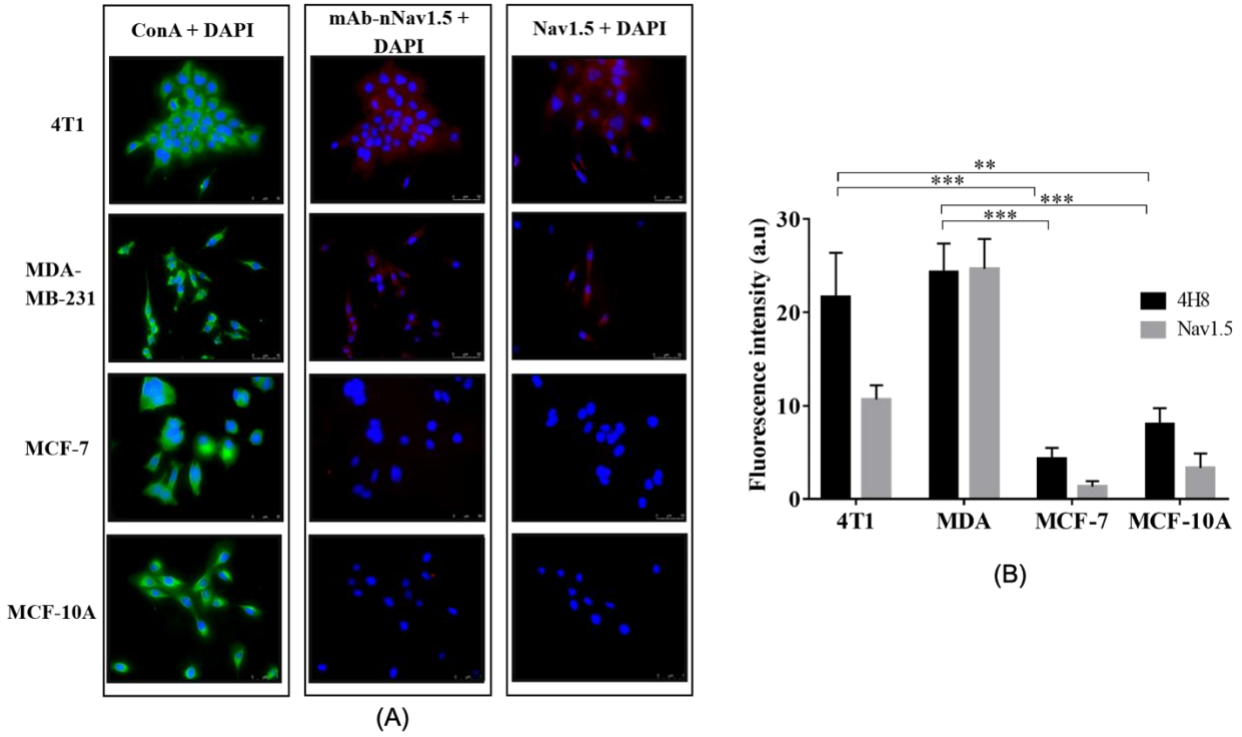

Figure 5. Immunoreactivity of 4H8 mAb-nNav1.5 compared to commercial anti-Nav1.5 mAb on fixed cells with different nNav1.5/Nav1.5 expression status. (A) Immunofluorescence microscopy images of 4T1, MDA-MB-231, MCF-7 and MCF-10A with 4H8 mAb-nNav1.5 and commercial anti-Nav1.5 antibody. (B) The graph shows the fluorescence intensity measurement of 4H8 mAb-nNav1.5 (black) and anti-Nav1.5 commercial antibody (grey), corrected to background values from the respective panel of cell lines. Blue fluorescence represents nuclear staining by DAPI, and green fluorescence by ConA represents the plasma membrane staining. Red fluorescence represents nNav1.5/Nav1.5 staining by 4H8 mAb-nNav1.5/commercial anti-Nav1.5 antibody; secondary antibody conjugated-Alexa Fluor 555. Images were viewed using Leica Inverted DMi8 fluorescence microscope, Leica Application Software X (LAS X) and captured using DFC 365 FX Camera (Leica Microsystems, Germany) at 40X magnification. Data were collected from n=3 independent experiments, presented as mean ± SEM. Tukey's Multiple Comparison Test was used, $p<0.01$, *** was considered statistically significant.

DISCUSSION

NESOpAb was the first anti-peptide pAb generated and demonstrated to recognise nNav1.5. The antibody immunoreactively proven by Western blotting produces signals against the heart and brain tissue homogenates of neonate mice but not the respective tissues of adult mice (Chioni *et al.*, 2005). Also, on engineered EBNA-293 cells stably expressing nNav1.5, NESOpAb exhibited strong immunoreactivity of immunofluorescence staining, in contrast to native EBNA cells (control) and those transfected with the 'adult' Nav1.5 where no immunoreactivity was observed (Chioni *et al.*, 2005). Additionally, consistent with mRNA expression data (MDA-MB-231 has been reported to express >100-fold higher VGSC mRNA compared to MCF-7 cells (Brackenbury *et al.*, 2007)), NESOpAb was able to demonstrate that nNav1.5 protein was abundantly expressed in MDA-MB-231 cells, which is known for its aggressive capacity but not the less aggressive, MCF-7 cells, which is known for its less-aggressive capacity (Brackenbury *et al.*, 2007). Subsequently, NESOpAb has enabled most investigations to understand nNav1.5's role in breast cancer metastasis (Brackenbury *et al.*, 2007). Currently, a commercialised antibody, 4G8:1G7

(Abcam), is claimed to bind against nNav1.5; however, a new and improved 'tool' to study nNav1.5 expression and its role in disease is needed. In the current study, the same published specific-linear peptide sequence of nNav1.5 – VSENIKLGNLSALRC was used to raise polyclonal NESOpAb in rabbits (Chioni *et al.*, 2005), was utilised as an immunogen for immunisation in generating monoclonal antibody (mAb) in mice. The motivation to generate mAb was driven by the ambition of having a homogenous antibody that interacts with a particular epitope on the nNav1.5 hence, more specific recognition is produced.

Screening of animals' serum antibody response after immunisation using ELISA identified serum from immunised C57BL/6 strain was the best; therefore, proceeded for spleen extraction. The result was anticipated since the strain is notable for its initial strain development goal; its use in the study of cancer and immune (Song & Hwang, 2017). Subsequent fusion of splenocytes with myelomas produced 20 hybridoma clones. Following screening by ELISA and Western blotting, finally, clone 4H8 was identified as the best clone for purification.

The purified mAb-nNav1.5 from 4H8 was characterised for its efficacy against the nNav1.5 short linear peptide using ELISA and SPR, against cell and tissue lysates using Western blotting and against intact fixed cells using immune fluorescence staining. In ELISA, the generation of linear association against the nNav1.5 specific-linear sequence of amino acids was achieved. Similarly, the results were reproducible when measured using SPR. These findings support the ability of the 4H8 mAb-nNav1.5 for nNav1.5 detection and quantitative measurement. When the purified 4H8 mAb-nNav1.5 was used against lysates of cells (human breast cancer MDA-MB-231 and MCF-7 cells and 4T1 mouse mammary tumour cells) and lysates of tumour tissue (4T1-induced mouse orthotopic syngeneic mammary tumour model) using Western blotting, the 4H8 mAb-nNav1.5 unable to produce specific protein band with approximate size for nNav1.5 (>220 kDa). On the contrary, for immunofluorescence microscopy, cells shown to express nNav1.5 abundantly, MDA-MB-231 and 4T1 were prominently stained by 4H8 mAb-nNav1.5 and almost non-visible in cells known to lack and absence of nNav1.5 expression, MCF-7 and MCF-10A, respectively. A similar observation was seen with the commercial anti-Nav1.5. The ability of the antibody to detect nNav1.5 in intact fixed cells could indicate that the obtained antibody was suitable for fluorescence microscopy but not Western blotting assay. This is common even in commercialised antibodies, where some antibody only indicated for certain assays. Furthermore, it is also important to note that nNav1.5 mRNA can be detected by real-time PCR in human and mouse cells and sequencing of the PCR product confirmed that nNav1.5 in human and mouse to be similar (data not shown). It is expected that 4H8 mAb-nNav1.5 could be immunoreactive to both human and mouse samples per the previously reported rabbit polyclonal NESOpAb, where NESOpAb is also able to immunoreact on mouse tissue and human breast cancer cells (Chioni *et al.,* 2005; Brackenbury *et al.,* 2007). Our ongoing work is to test 4H8 mAb-nNav1.5 utilisation in immunohistochemistry on patient tissue; immunofluorescence staining on nNav1.5-knockdown and overexpressing cells; and Western blot on tissue lysates of 'neonate' and 'adult' mice heart, comparing 4H8 mAb-nNav1.5 with other commercialised antibodies.

CONCLUSION

This study indicates the initial characterisation of 4H8 mAb-nNav1.5. For now, 4H8 mAb-nNav1.5 can be utilised to measure nNav1.5 using ELISA and detect cells expressing nNav1.5 using fluorescence microscopy.

ACKNOWLEDGEMENTS

This study was supported and funded by the Ministry of Education, Malaysia through the Higher Institution Centre of Excellence (HICoE) Program (No. 311/CIPPM/4401005) and the Fundamental Research Grant Scheme (FRGS/1/2018/SKK08/USM/03/2). Also the Ministry of Science, Technology and Innovation, Malaysia, under the Science Fund (Grant no: 06-01-05-SF0844). We also thank Madam Amy

Amilda Anthony for technical support during ELISA experiments.

CONFLICT OF INTEREST

The authors have declared that no conflict of interest exists.

REFERENCES

Abcam. 2015. Available at: https://www.abcam.com/nnav15-antibody-4g81g7-ab62388.html.

Angus M., & Ruben P. 2019. Voltage gated sodium channels in cancer and their potential mechanisms of action. *Channels* 13(1): 400–409.

Black J. A., & Waxman S. G. 2013. Non-canonical roles of voltage-gated sodium channels. *Neuron* 80(2): 280–291.

Brackenbury W. J., Chioni A. M., Diss J. K., & Djamgoz M. B. A. 2007. The neonatal splice variant of Nav1.5 potentiates in vitro invasive behaviour of MDA-MB-231 human breast cancer cells. *Breast Cancer Research and Treatment* 101(2): 149–160.

Chioni A. M., Fraser, S. P., Pani, F., Foran, P., Wilkin, G. P., Diss, J. K., & Djamgoz, M. B. 2005. A novel polyclonal antibody specific for the Nav1.5 voltage-gated Na^+ channel "neonatal" splice form. *Journal of Neuroscience Methods* 147(2): 88–98.

Fraser S. P., Diss, J. K., Chioni, A. M., Mycielska, M. E., Pan, H., Yamaci, R. F., Pani, F., Siwy, Z., Krasowska, M., Grzywna, Z., & Brackenbury, W. J. 2005. Voltage-gated sodium channel expression and potentiation of human breast cancer metastasis. *Human Cancer Biology* 11(15): 5381–5389.

Gazina E. V., Richard, K. L., Mokhtar, M. B. C., Thomas, E. A., Reid, C. A., & Petrou, S. 2010. Differential expression of exon 5 splice variants of sodium channel α subunit mRNAs in the developing mouse brain. *Neuroscience* 166(1): 195–200.

Guo L., Abrams, R. M., Babiarz, J. E., Cohen, J. D., Kameoka, S., Sanders, M. J., Chiao, E., & Kolaja, K. L. 2011. Estimating the risk of drug-induced proarrhythmia using human induced pluripotent stem cell-derived cardiomyocytes. *Toxicological Sciences* 123(1): 281–289.

Guzel R. M., Ogmen, K., Ilieva, K. M., Fraser, S. P., & Djamgoz, M. B. 2019. Colorectal cancer invasiveness in vitro: Predominant contribution of neonatal Nav1.5 under normoxia and hypoxia. *Journal of Cellular Physiology* 234(5): 6582–6593.

Hille, B. 2001. Potassium channels and chloride channels. *Ionic Channels of Excitable Membranes*: 131–168.

Hucho, F. 2019. Ion channels in excitable membranes. *Transport by Proteins*. Berlin. Boston. De Gruyter: 221–240.

Kamarulzaman N. S., Dewadas, H. D., Leow, C. Y., Yaacob, N. S., & Mokhtar, N. F. 2017. The role of REST and HDAC2 in epigenetic dysregulation of Nav1.5 and nNav1.5 expression in breast cancer. *Cancer Cell International* 17(1): 74.

Mao W., Zhang, J., Körner, H., Jiang, Y., & Ying, S. 2019. The emerging role of voltage-gated sodium channels in tumor biology. *Frontiers in Oncology* 9(124): 1–8.

Nelson M., Yang M., Millican-Slater R., & Brackenbury W. J. 2015. Nav1.5 regulates breast tumor growth and metastatic dissemination *in vivo*. *Oncotarget* 6(32): 32914–32929.

Nelson M., Yang M., Dowle A. A., Thomas, J. R., & Brackenbury, W. J. 2015. The sodium channel-blocking antiepileptic drug phenytoin inhibits breast tumour growth and metastasis. *Molecular Cancer* 14(1): 1–7.

Rosas-Arellano A., Villalobos-González, J. B., Palma-Tirado., L., Beltrán, F. A., Cárabez-Trejo, A., Missirlis, F., & Castro, M. A. 2016. A simple solution for antibody signal enhancement in immunofluorescence and triple immunogold assays. *Histochemistry and Cell Biology* 146(4): 421–430.

Schroeter A., Walzik, S., Blechschmidt, S., Haufe, V., Benndorf, K., & Zimmer, T. 2010. Structure and function of splice variants of the cardiac voltage-gated sodium channel Nav1.5. *Journal of Molecular and Cellular Cardiology* 49(1): 16–24.

Song H. K., & Hwang D. Y. 2017. Use of C57BL/6N mice on the variety of immunological researches. *Laboratory Animal Research* 33(2): 119.

Terlau H., & Kirchhoff F. 2006. Ion channels/excitable membranes. *Encyclopedic Reference of Genomics and Proteomics in Molecular Medicine*: 913–916.

Utrilla R. G., Nieto-Marín, P., Alfayate, S., Tinaquero, D., Matamoros, M., Pérez-Hernández, M., Sacristán, S., Ondo, L., De Andres, R., Díez-Guerra, F. J., & Tamargo, J. 2017. Kir2.1-Nav1.5 channel complexes are differently regulated than Kir2.1 and Nav1.5 channels alone. *Frontiers in Physiology* 8(11): 1–16.

Vikram A., Lewarchik, C. M., Yoon, J. Y., Naqvi, A., Kumar, S., Morgan, G. M., Jacobs, J. S., Li, Q., Kim, Y. R., Kassan, M., & Liu, J. 2017. Sirtuin 1 regulates cardiac electrical activity by deacetylating the cardiac sodium channel. *Nature Medicine* 23(3): 361–367.

Xing D., Wang, J., Ou, S., Wang, Y., Qiu, B., Ding, D., Guo, F., & Gao, Q. 2014. Expression of neonatal Nav1.5 in human brain astrocytoma and its effect on proliferation, invasion and apoptosis of astrocytoma cells. *Oncology Reports* 31(6): 2692–2700.

Yang M., Kozminski, D. J., Wold, L. A., Modak, R., Calhoun, J. D., Isom, L. L., & Brackenbury, W. J. 2012. Therapeutic potential for phenytoin: Targeting Nav1.5 sodium channels to reduce migration and invasion in metastatic breast cancer. *Breast Cancer Research and Treatment* 134(2): 603–615.